

# Impulse Noise Mitigation Based on Computational Intelligence for Improved Bit Rate in PLC-DMT

Moisés V. Ribeiro, *Member, IEEE*, Renato da R. Lopes, João Marcos T. Romano, *Senior Member, IEEE*, and Carlos A. Duque, *Member, IEEE*

**Abstract**—This paper introduces a modified version of the discrete multi-tone transceiver (DMT) to increase the data rate in broadband power-line communications (PLC). Basically, a computational-intelligence technique trained by a second-order optimization method is applied to mitigate the high-power impulse noise, while the DMT copes with the severe intersymbol interference observed in power-line channels. The masking of the impulse noise enhances the signal-to-noise ratio in each DMT subchannel. As a result, a high number of bits can be allotted to each subchannel for a given error probability. The simulation results reveal that the proposed PLC-DMT solution outperforms, in terms of the data rate, traditional PLC-DMT over different environments, especially in the presence of additive high-power impulse noise.

**Index Terms**—Communication systems, data communication, frequency-division multiplexing, impulse noise, multipath channels, neural networks, power system communication.

## I. INTRODUCTION

POWER-LINE (PL) networks have recently been studied as a medium for broadband transmission of Internet contents, for the usage of new multimedia services (video on demand, audio distribution, multiplayer gaming, HDTV, telephony, and teleconferencing) and for the connection of peripherals (printers and scanners) to a computer. This is a new paradigm for the power-line grids, which were initially developed for energy delivery at frequencies of 50 or 60 Hz, and only recently employed in narrowband applications such as control, maintenance, and charging by the utility companies [1].

Power-line communications (PLC) is a no-new-wires network that provides convenient and widespread networking services such as the ones previously mentioned. In this context, PL networks compete against cable and phone line networks. In fact, it has been shown that transmissions through low, medium, and rural voltage grids are as good as digital subscriber line (DSL) and cable TV channels to provide high-rate data trans-

missions [2]–[8]. Besides, PLC may also compete with wireless networks such as 802.11x in the market for high-rate in-home (indoor) and local-access (outdoor) networks [3].

It has been recognized that PL channels are hostile environments for data transmission [1]–[10]. Varying impedances, high-power impulse noise, multiple-access interference, and multipath frequency-selective fading, in addition to time-, frequency-, distance-, and location-dependent attenuations are their main problems. Moreover, the coupling problem related to power-line and PLC modems is also another source of impairment. Several signal-processing techniques have been applied to overcome such impairments [9]–[13].

Impulse noise is probably one of the most serious impairments introduced by PL channels, since it can corrupt a burst of transmitted information. However, this impairment has not been well addressed in the literature. In fact, most of the signal processing techniques developed for PLC applications have assumed the noise to be Gaussian and, as a result, incur significant performance degradations when applied to PL channels corrupted by impulse noise.

Discrete multi-tone transceivers (DMTs) based on the orthogonal frequency-division multiplexing (OFDM) concept have been shown to be a powerful tool for reducing severe intersymbol interference (ISI) that occurs in broadband PLC applications [10], [11], [20]. Unfortunately, none of the proposed robust signal processing techniques are capable of coping with both the impulse noise and ISI.

This contribution presents a modified PLC-DMT solution [31], in which a nonlinear algorithm based on computational intelligence [14] is introduced to mask the non-Gaussian noise while channel shortening and OFDM are applied to deal with the ISI. It is shown through simulations that the proposed technique achieves a higher bit rate in the presence of impulse noise than that achieved in using the traditional techniques which assume a Gaussian noise interference.

The remainder of this paper is organized as follows. Section II provides a brief review of PLC, brings up the idea behind PLC-DMT solutions, and presents the PLC-DMT model and notation. Section III describes the proposed modified PLC-DMT solution. Section IV reports some simulation results of the proposed solution. Finally, some concluding remarks and points to possible directions for future works are included in Section V.

## II. PLC-DMT: SYSTEM DESCRIPTION

By the late 1980s, PLC became a reality with the development of high-performance coding and modulation techniques.

Manuscript received April 5, 2004; revised November 12, 2004. This work was supported in part by CAPES under Grant BEX2418/03-7, in part by CNPq under Grants 552371/01-7 and 150064/2005-5, and in part by FAPESP under Grants 01/08513-0 and 02/12216-3, all from Brazil. Paper no. TPWRD-00158-2004.

M. V. Ribeiro was with the Department of Communications, University of Campinas, Campinas SP 13 081 970, Brazil. He is now with the Department of Electrical Circuit, Federal University of Juiz de Fora, Juiz de Fora MG 36 036 330, Brazil (e-mail: mribeiro@ieee.org).

R. da Rocha Lopes, and J. Marcos T. Romano are with the Department of Communications, University of Campinas, Campinas SP 13 081 970, Brazil (e-mail: rlopes@decom.fee.unicamp.br; romano@decom.fee.unicamp.br).

C. A. Duque is with the Department of Electrical Circuit, Federal University of Juiz de Fora, Juiz de Fora MG 36 036 330, Brazil (e-mail: carlos.duque@ufjf.edu.br).

Digital Object Identifier 10.1109/TPWRD.2005.852271

Low-data-rate PLC modems were developed and applied to very short distances with very low bit rates. In recent years, researchers have been focusing on data rates higher than 50 Mb/s. This bit rate is still below the theoretical capacity of PLC, which is known to be higher than 500 Mb/s [7], [8]. However, a successful PLC system must meet several technical challenges. In fact, the power-line grid may severely corrupt the transmitted streams of data, mostly because it was devised for nothing but electrical low-loss power transportation at 50 or 60 Hz. Furthermore, PL channels have several discontinuities due to impedance mismatches. In addition, although the PL response hardly varies over time, at certain moments, it can change abruptly due to changes in the load distribution on the line.

The cable length, cable type, and degree of branching characterize the transfer function between two points of a specific power line. For modeling the transfer characteristics of power lines, two approaches can be applied, namely, the bottom up and the top down. The first describes the behavior of a power-line network by using parameter matrices of the network components. The latter considers the communication channel as a black box and describes its transfer characteristics by a transfer function. Fig. 1 shows the frequency response of three PL channels of different low-voltage distribution networks (LVDNs) based on the top-down approach [7], [17]. Frequency-selective property of the PL channel can be seen in this figure.

Some studies point out that outdoor PL channels of low- and medium-voltage grids occupy the frequency band from 1 to 10 MHz, while the indoor PL channels cover the frequency range from 10 to 30 MHz [7], [21]. For both frequency bands, the noise is modeled as an additive contribution whose components are [22]

$$\eta(n) = \eta_{\text{bkgr}}(n) + \eta_{\text{nb}}(n) + \eta_{\text{pa}}(n) + \eta_{\text{ps}}(n) + \eta_{\text{imp}}(n) \quad (1)$$

where  $\eta_{\text{bkgr}}(n)$  is the background Gaussian noise,  $\eta_{\text{nb}}(n)$  is narrowband noise,  $\eta_{\text{pa}}(n)$  is a periodic impulse noise asynchronous to the fundamental component of the power system,  $\eta_{\text{ps}}(n)$  is a periodic impulse noise synchronous to the fundamental component of the power system, and  $\eta_{\text{imp}}(n)$  is an asynchronous impulse noise. In this contribution, we consider only the presence of asynchronous impulse noise, because it is the hardest problem for broadband PLC and, as a result, for our analysis, we assume the noise model to be of the form

$$\eta(n) = \eta_{\text{bkgr}}(n) + \eta_{\text{imp}}(n). \quad (2)$$

It is well known that the multicarrier transmission is a high-performance, low-complexity solution when the channel is corrupted by ISI and linear additive white Gaussian noise [18], [19]. Although the noise in the power-line grid is not accurately modeled as additive white Gaussian noise, several contributions have reported that multicarrier techniques are also well suited for PLC [9], [11], [20]. Fig. 2 shows a DMT system scheme, to be called PLC-DMT, that focuses on achieving high data rates in the LVDN for broadband Internet-access networks. As can be seen in Fig. 2, this is the same scheme that is used in xDSL applications [11], [19], [20]. Consider the transmission of a discrete-time signal  $x(n)$  through a linear dispersive PL channel

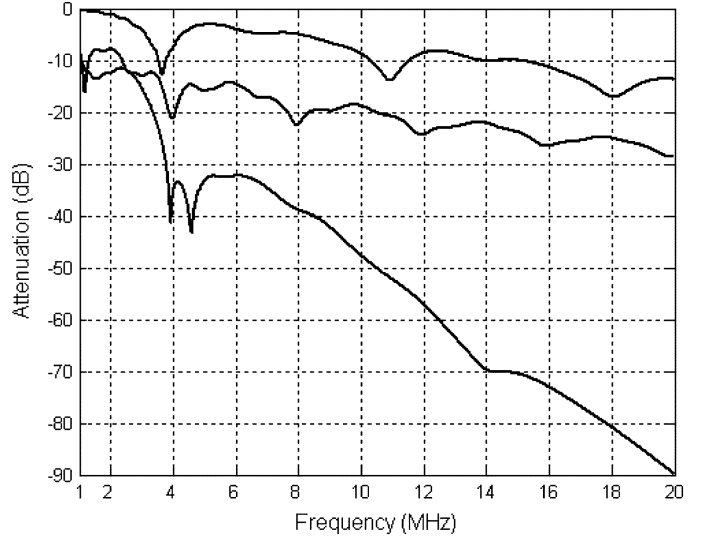


Fig. 1. PL characteristic of three LVDNs.

whose discrete impulse response is given by  $\{h(n)\}_{n=0}^{L_h-1}$ . The channel output is then given by

$$y(n) = \tilde{y}(n) + \eta(n) = \sum_{k=0}^{L_h-1} h(k)x(n-k) + \eta(n) \quad (3)$$

where  $\tilde{y}(n)$  takes into account the effect of the ISI and  $\eta(n)$  is the additive non-Gaussian noise at the output of the PL channel.

In OFDM systems, the signal  $x(n)$  is computed and transmitted in blocks, so the whole discrete time system can be understood in a matrix formulation as follows. Let  $\mathbf{S}_1 = [S(0) \cdots S((N/2) - 1)]^T$  be the block of encoded symbols to be transmitted. The OFDM transmitter then forms the vector  $\mathbf{S}_a = [S_a(0) \cdots S_a(N-1)]^T$ , with elements  $S_a(k)$ ,  $k = 0, \dots, N-1$  given by

$$S_a(k) = \begin{cases} S_1(k), & k = 1, \dots, N/2 - 1, \\ \Re(S_1(N/2)), & k = 0, \\ \Im(S_1(N/2)), & k = N/2, \\ S_1^*(k - N/2), & k = N/2 + 1, \dots, N - 1 \end{cases} \quad (4)$$

where  $\Re[S_1(k)]$  and  $\Im[S_1(k)]$  are, respectively, the real and imaginary components of the  $k$ th element of the vector  $\mathbf{S}_1$ . Next, the vector  $\mathbf{x} = [x(0) \cdots x(N-1)]^T = \mathbf{Q}^* \mathbf{S}_a$ , known as the OFDM symbol, is computed, where  $\mathbf{Q}^*$  denotes the  $N \times N$  inverse discrete Fourier transform (IDFT) matrix. The transmitted vector is then  $[x(0) \cdots x(N-1) \ x(0) \cdots x(v-1)]^T$ . It should be noted that  $v \geq L_c - 1$  is the length of cyclic prefix added to each transmitted OFDM symbol for the reason that it will become apparent shortly, and  $L_c$  is the length of equivalent channel impulse response  $\mathbf{c} = \mathbf{h} * \mathbf{w} = [c(0) \cdots c(L_c - 1)]^T$ .

Now, let  $\boldsymbol{\eta} = [\eta(v) \cdots \eta(N+v-1)]^T$  denote the noise vector,  $\mathbf{W}$  denote the convolution matrix of the channel-shortening time-domain equalizer (TEQ) with an impulse response given by  $\mathbf{w} = [w_0 \cdots w_{L_w-1}]^T$ , and  $\mathbf{C}$  denotes the convolution matrix of the equivalent channel impulse response  $\mathbf{c}$ . Also, let  $\mathbf{r} = [r(v) \cdots r(N+v-1)]^T$  be a vector formed with the final  $N$  samples of the TEQ output. Then, we can write  $\mathbf{r} = \mathbf{C}\mathbf{x} + \mathbf{W}\boldsymbol{\eta}$ .

It is well known that if a cyclic prefix is added to a sequence, which is transmitted through a discrete-time system with an

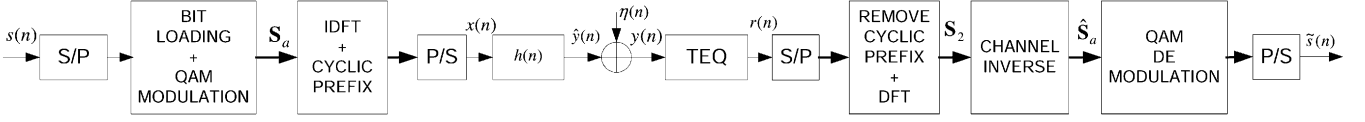


Fig. 2. Conventional PLC-DMT scheme (S/P: serial to parallel).

impulse response  $\{b(n)\}_{n=0}^{L_b-1}$ , then the convolution matrix of  $\{b(n)\}_{n=0}^{L_b-1}$ , which we call  $\mathbf{B}$ , turns out to be a cyclic matrix and its eigenvectors are the basis vectors of the discrete Fourier transform (DFT) [16]. Assuming that  $\mathbf{C}$  is circular (i.e., that the effective length of the equivalent channel response is given by  $L_c \leq v + 1$  [15], [16]), we get

$$\begin{aligned} \mathbf{S}_2 &= \mathbf{Q}\mathbf{r} = \mathbf{Q}(\mathbf{Q}^* \mathbf{\Lambda}_C \mathbf{Q})\mathbf{x} + \mathbf{Q}(\mathbf{W}\boldsymbol{\eta}) \\ &= \mathbf{\Lambda}_C \mathbf{Q}\mathbf{x} + \mathbf{N} = \mathbf{\Lambda}_C \mathbf{S}_a + \mathbf{N} \end{aligned} \quad (5)$$

where  $\mathbf{S}_2$  is a  $N \times 1$  vector,  $\mathbf{Q}$  is the  $N \times N$  DFT matrix,  $\mathbf{\Lambda}_C$  is a diagonal matrix, whose values are the DFT coefficients of the impulse response vector  $\mathbf{c}$ , and  $\mathbf{N} = \mathbf{Q}\mathbf{W}\boldsymbol{\eta}$  is the DFT of the additive non-Gaussian noise vector  $\boldsymbol{\eta}$ . It is clear from (5) that the transmitted symbols can then be recovered as

$$\hat{\mathbf{S}}_a = (\mathbf{\Lambda}_C)^{-1} \mathbf{S}_2 = \mathbf{S}_a + (\mathbf{\Lambda}_C)^{-1} \mathbf{N}. \quad (6)$$

The sequence  $\hat{\mathbf{S}}_1$ , which is delivered to the quadrature amplitude modulation (QAM) demodulation block, is obtained after applying the inverse of the operation performed by (4)–(6). We next discuss a modified version of the PLC-DMT that addresses the presence of the non-Gaussian noise in the second term on the right-hand side (RHS) of (6).

### III. PROPOSED MODIFIED PLC-DMT (M-PLC-DMT) SCHEME

From (5) and the fact that  $\mathbf{\Lambda}_C$  is diagonal, it is clear that as long as the matrix  $\mathbf{C}$  is circular, the DMT system can be seen as being composed of several intersymbol interference (ISI)-free subchannels, each of which is subject to a different gain and a different noise term with power given by

$$S_{\eta,i} = S_{\text{bkgr},i} + S_{\text{imp},i}. \quad (7)$$

However, the assumption that the matrix  $\mathbf{C}$  is circular does not hold exactly, since the channel-shortening equalizer is usually not able to perfectly reduce the length of the overall impulse response to less than  $v$ . Thus, the  $i$ th subchannel is subject to some residual ISI, whose power is given by [24]

$$I_i = S_{x,i} |C_i^{\text{ISI}}|^2 \quad (8)$$

where  $S_{x,i}$  and  $|C_i^{\text{ISI}}|^2$  are the power of the transmitted signal and the ISI path gain [24], respectively. A subchannel signal-to-

noise ratio (SNR) that takes into account both the noise power and the residual ISI power is defined by [24]

$$\Omega_i = \frac{S_{x,i} |C_i^{\text{SIGNAL}}|^2}{S_{\eta,i} |W_i^{\text{NOISE}}|^2 + S_{x,i} |C_i^{\text{ISI}}|^2} \quad (9)$$

where  $|C_i^{\text{SIGNAL}}|^2$  and  $|W_i^{\text{NOISE}}|^2$  are the  $i$ th signal path gain and the  $i$ th noise path gain, respectively. The equivalent path gain vectors are the diagonal entries of  $\mathbf{\Lambda}_C$ . It can be shown that the achievable bit rate of a DMT system is an increasing function of this SNR, so that the higher the SNR is, the higher the bit rate [24].

From (9), it can be seen that in the presence of non-Gaussian noise, a lower SNR is attained in each  $i$ th subchannel, decreasing the achievable bit rate. Moreover, a low SNR can disturb the evaluation of the channel-shortening equalizer  $\mathbf{w}$ , leading to a suboptimal solution regardless of the criterion used in the equalizer design. This leads to increased ISI power, further decreasing the achievable bit rate. Since all of the terms in (9) are positive, it is clear that a signal processing method that mitigates the impulse noise components will decrease the noise power  $S_{\eta,i}$ . Moreover, if this method does not affect the other signal and noise components, the result will be increased SNR in (9) and, thus, an increased bit-rate capacity and an improved computation of the TEQ. The use of a suitable method that completely reduces  $S_{\text{imp},i}$  will lead to a new SNR given by (10), shown at the bottom of the page, in the  $i$ th subchannel, where  $K_i$  denotes the attenuation of the impulse noise attained by using this method.

With this objective, Fig. 3 portrays the proposed modified PLC-DMT (M-PLC-DMT), where the non-Gaussian noise mitigation (NNM) is implemented with a technique that evolves from computational intelligence, as discussed later.

In Fig. 3, the OFDM and the channel-shortening equalizer contend with the ISI. The next section discusses the multilayer perceptron neural network (MLPNN) as a particular case of a computational intelligence technique for the reduction of the non-Gaussian noise.

#### A. Computational Intelligence Based on the Nonlinear Technique for Impulse Noise Mitigation

The majority of computational intelligence techniques can be derived from a unique mathematical formulation [14]. As

$$\begin{aligned} \bar{\Omega}_i &= \frac{S_{x,i} |C_i^{\text{SIGNAL}}|^2}{K_i \left( S_{\text{imp},i} |W_i^{\text{NOISE}}|^2 \right) + S_{\text{bkgr},i} |W_i^{\text{NOISE}}|^2 + S_{x,i} |C_i^{\text{ISI}}|^2} \Bigg|_{K_i=0} \\ &= \frac{S_{x,i} |C_i^{\text{SIGNAL}}|^2}{S_{\text{bkgr},i} |W_i^{\text{NOISE}}|^2 + S_{x,i} |C_i^{\text{ISI}}|^2} \end{aligned} \quad (10)$$

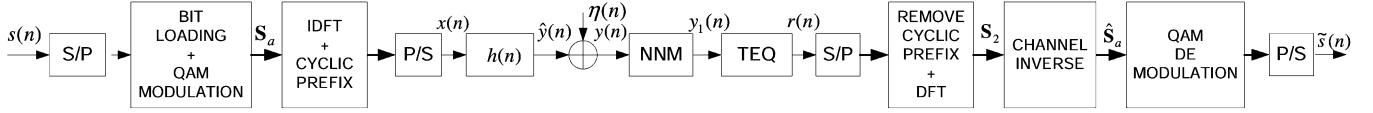


Fig. 3. Modified PLC-DMT scheme.

a result, it is possible to train either neural networks (NNs) or wavelet networks (WNs), learning from the experience of human operators expressed in terms of linguistic rules; or to interpret, in linguistic form, the knowledge that either an NN or a WN has been acquired from prior examples. It is also possible to train, with a unique training rule, hybrid systems composed of different computational intelligence techniques [14]. Due to the aforementioned characteristics, these techniques have been widely applied to solve many nonlinear problems. In fact, the ability of such techniques to learn nonlinear features from the available data have provided new perspectives for classification, recognition, detection, and removal of signals corrupted by the nonlinear component.

Considering that the impulse noise is a nonlinear component, we apply an MLPNN with one hidden layer inside the NNM block to remove the impulse noise from the output of the PL channels. If and only if the MLPNN is able to completely remove the impulse noise, the input of the TEQ block, which implement a TEQ technique, will have an SNR value given by

$$\bar{\Omega}_{\text{TEQ}} = \frac{\sigma_{\tilde{y}}^2}{\sigma_{\text{bkgr}}^2} \quad (11)$$

where  $\sigma_{\tilde{y}}^2$  and  $\sigma_{\text{bkgr}}^2$  are the power of the noise-free channel output  $\tilde{y}(n)$  defined in (3) and the background noise given in (1), respectively. As a result, the new  $i$ th SNR value defined in (10) can be achieved. Note that the SNR value at the input of the TEQ block in the PLC-DMT is given by

$$\Omega_{\text{TEQ}} = \frac{\sigma_{\tilde{y}}^2}{\sigma_{\text{bkgr}}^2 + \sigma_{\text{imp}}^2} \leq \bar{\Omega}_{\text{TEQ}} \quad (12)$$

where  $\sigma_{\text{imp}}^2$  is the power of the impulse noise. The use of a nonlinear technique in the NNM block instead of a linear one is due to the fact that the latter, being linear, cannot change intrinsic properties of the original noise signal, such as regularity [25]. In addition, linear techniques are not well suited to suppress the additive non-Gaussian noise when the signal is wideband and nonstationary [25].

To obtain an efficient MLPNN, we use a modified version of the scaled conjugated gradient (MVSCG) optimization method [26]. The motivation for using this training method is that the MVSCG is one of the most efficient second-order optimization methods for the training of the artificial neural networks (ANNs) [26], [27]. It is worth stressing that in this proposed modification, it is assumed that the channel has been previously estimated and that a training sequence is available in the receiver for training the NNM. The state space formulation of an MLPNN with one hidden layer is given by [27]

$$\mathbf{z}(n) = \mathbf{A}^T(n)\mathbf{y}(n), \quad (13)$$

$$\mathbf{u}(n) = \mathbf{f}(\mathbf{z}(n)) = [f(z_0(n)) \cdots f(z_{I-1}(n))]^T \quad (14)$$

$$y_1(n) = \mathbf{b}^T(n) \begin{bmatrix} \mathbf{u}(n) \\ 1 \end{bmatrix}, \quad (15)$$

$$f(z_i(n)) = \tanh(z_i(n)), \quad i = 1, \dots, I \quad (16)$$

where  $\mathbf{y}(n) = [y(n) \cdots y(n-K+1) 1]^T$  is the  $(K+1) \times 1$  input vector, which is constituted by samples of the output channel as defined in (3) and the bias of the MLPNN;  $\mathbf{z}(n) = [z_0(n) \cdots z_{I-1}(n)]^T$  is the neuron output vector in the hidden layer;  $I$  is the number of neurons in the hidden layer;  $y_1(n)$  is the NN output;  $\mathbf{A}(n) \in \mathfrak{R}^{(K+1) \times I}$  is the matrix of weights between the input and the hidden layers; and  $\mathbf{b}(n) \in \mathfrak{R}^{(I+1) \times 1}$  is the matrix of weights between the hidden and the output layer.

Let  $\mathbf{a}(n)$  be a column vector formed by the columns of the matrix  $\mathbf{A}(n)$ . Then, the vector  $\mathbf{p}(n)$  containing all weights of the MLPNN; the error measure  $E(\mathbf{p}(n))$ ; the total error measure  $E_T(\mathbf{p}(n))$  for a set of training data; and the gradient vector  $\nabla E_T(\mathbf{p}(n))$  are given by

$$\mathbf{p}(n) = [\mathbf{a}^T(n) \quad \mathbf{b}^T(n)]^T \quad (17)$$

$$E(\mathbf{p}(n)) = \frac{1}{2}e(n)^2 = \frac{1}{2}(\tilde{y}(n) - y_1(n))^2 \quad (18)$$

$$E_T(\mathbf{p}(n)) = \sum_n E(\mathbf{p}(n)) \quad (19)$$

$$\nabla E_T(\mathbf{p}(n)) = [\nabla E_{\mathbf{a}}^T(n) \quad \nabla E_{\mathbf{b}}^T(n)]^T \quad (20)$$

respectively, where  $\tilde{y}(n)$  is the desired output;  $e(n)$  is the output error; and  $\nabla E_{\mathbf{a}}(n)$  and  $\nabla E_{\mathbf{b}}(n)$  are the gradients of the error measure with respect to  $\mathbf{a}(n)$  and  $\mathbf{b}(n)$ , respectively. From the definition of the error measures in (18) and (19), it can be seen that the NN tries to make its output as close as possible to the noise-free channel output  $\tilde{y}(n)$  in a least-squares sense.

The implementation of the MVSCG optimization method [26], [27] makes use of the fast exact product of the Hessian matrix by directional vector as described in [28]. This combination leads to a low computational burden in the training procedure because the Hessian matrix is not directly evaluated.

The next section shows some simulations results that illustrate the feasibility of this technique.

#### IV. PERFORMANCE ANALYSIS

In this section, we compare the performance of the proposed M-PLC-DMT with that of a traditional PLC-DMT. As a performance measure in the simulations, we use the overall bit-rate defined by [16]

$$\text{bit rate} = \left( \sum_{i \in S} b_i \right) \frac{F_s}{N + v} \quad (21)$$

$$b_i = \left\lfloor \log_2(1 + 10^{(\text{SNR}_i - \Gamma - \gamma_m + \gamma_c)/10}) \right\rfloor \quad (22)$$

where  $b_i$  denotes the number of bits assigned to the  $i$ th sub-channel,  $F_s$  is the sample rate,  $N$  is the number of subchannels,  $\Gamma$  is the SNR gap,  $\gamma_m$  is the noise margin, and  $\gamma_c$  is the coding gain.

We used the following parameters in our simulations: background noise with a power spectral density (PSD) equal to  $-120$  dB/Hz; impulse noise with a PSD varying from  $-90$  to  $-105$  dB/Hz; transmitted OFDM symbols with a PSD equal to  $-70$

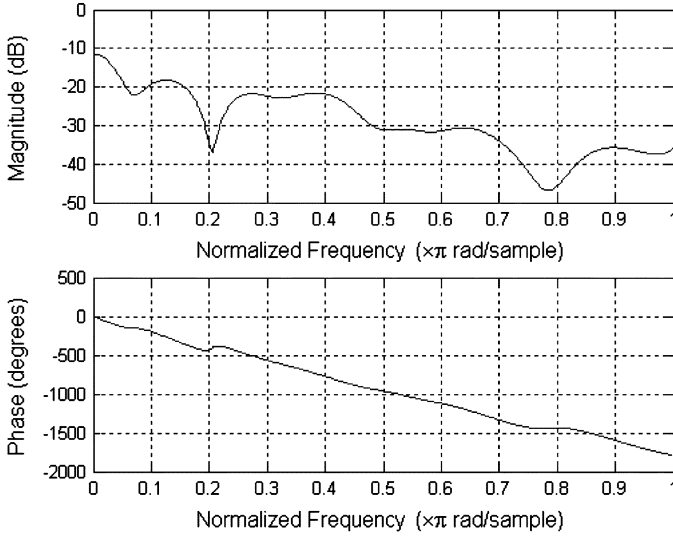


Fig. 4. PL channel 1: Frequency response.

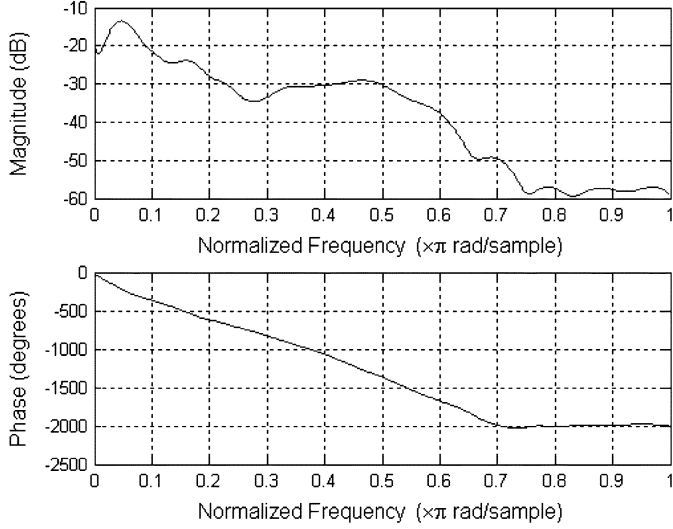


Fig. 5. PL channel 2: Frequency response.

dB/Hz; length  $N$  of the OFDM symbol equal to 2048; training OFDM symbols with flat energy over all subchannels [30]; the number of OFDM symbols used for the training of the NNM and the TEQ are equal to 50 and 350, respectively; the sampling frequency of  $F_s = 9.6$  MHz. The used MLPNN has one input, 18 neurons in its hidden layer, and one output, while the PLC-DMT signal is assumed to occupy the 0.2–5 MHz frequency range. The frequency responses of the LVDN PL channels are the same as in [17]. Figs. 4 and 5 depict the impulse responses of the PL channels used.

Figs. 6 and 7 show the channel output with and without the impulse noise, as well as the MLPNN output, for both PL channels. For these cases, the mean-squared errors obtained in the training are equal to  $-25.94$  and  $-28.63$  dB, respectively. In these plots, all signals have been submitted to a gain to clearly show the performance of the MLPNN. As can be seen in these figures, the MLPNN has successfully reduced the impulse noise at the output of both PL channels. In these specific simulations, the PSD of the transmitted signal is equal to  $-70$  dB/Hz, the

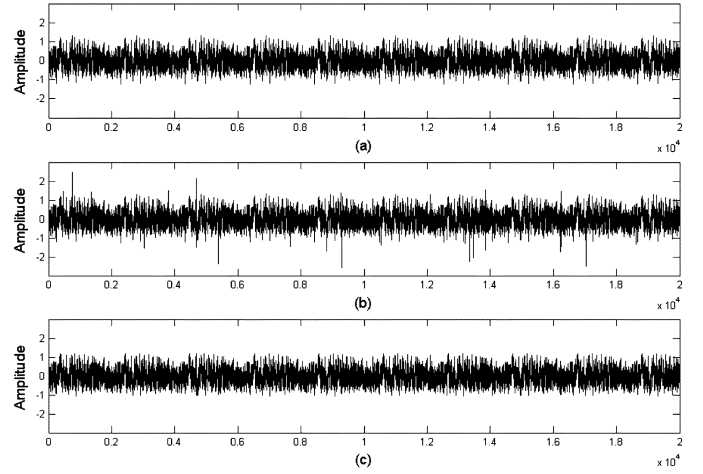


Fig. 6. (a) The channel output, (b) the channel output plus the additive non-Gaussian noise, and (c) the output of MLPNN. Refer to the PL channel 1.

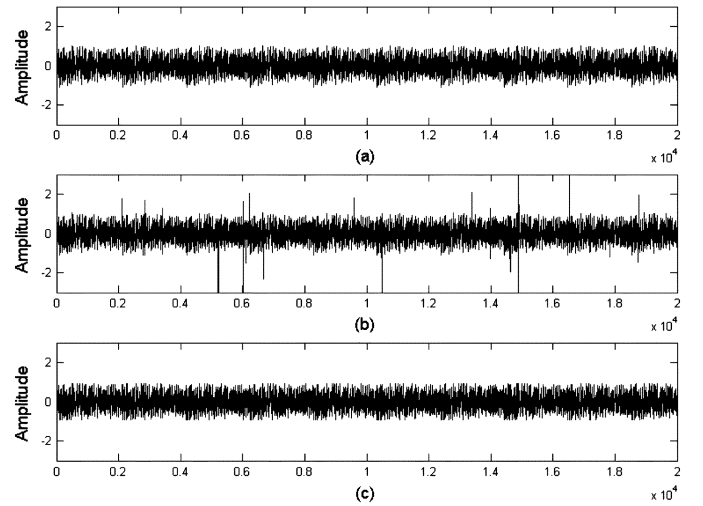


Fig. 7. (a) The channel output, (b) the channel output plus the additive non-Gaussian noise, and (c) the output of the MLPNN. Refer to the PL channel 2.

PSD of background noise is equal to  $-120$  dB/Hz, and the PSD of the impulse noise is equal to  $-90$  dB/Hz. For these results, it was considered that the length of the cyclic prefix  $v = 16$  and  $L_w$  is equal to 48 and 56 for PL channels 1 and 2, respectively.

As discussed in Section III, the masking of the impulse noise by the MLPNN results in an increased SNR in each subchannel. Numerical results verifying this behavior are given in Tables I and II, which show the SNR in the input of the TEQ block with (column marked PLC-DMT) and without (column marked M-PLC-DMT) an MLPNN, with different values for the impulse noise PSD. The SNR values shown in Tables I and II are given by

$$\text{SNR} = \frac{\sigma_y^2}{\sigma_{\eta}^2} \quad (23)$$

where  $\sigma_y^2$  and  $\sigma_{\eta}^2$  denote the desired signal power at the channel output and the noise power, respectively. As seen in these tables, the SNR improvement made possible by the MLPNN can exceed 5.5 dB.

TABLE I  
PL CHANNEL 1: SNR  $\times$  IMPULSE NOISE PSD

PSD (dB/Hz)	SNR (dB) PLC-DMT	SNR (dB) M-PLC-DMT
-90.0	14.22	18.26
-92.5	17.14	19.69
-95.0	18.89	20.42
-97.5	21.12	21.63
-100.0	22.79	23.02
-102.5	24.22	24.29
-105.0	25.17	25.19

TABLE II  
PL CHANNEL 2: SNR  $\times$  IMPULSE NOISE PSD

PSD (dB/Hz)	SNR (dB) PLC-DMT	SNR (dB) M-PLC-DMT
-90.0	12.29	18.09
-92.5	14.88	18.71
-95.0	18.97	20.21
-97.5	21.03	21.55
-100.0	20.45	20.98
-102.5	21.87	22.07
-105.0	22.95	23.01

TABLE III  
PL CHANNEL 1: M-PLC-DMT AND PLC-DMT PERFORMANCE UNDER DIFFERENT IMPULSE NOISE PSD LEVELS

PSD(dB/Hz)	Bit-rate (Mbps) PLC-DMT	Bit-rate (Mbps) M-PLC-DMT
-90.0	31.68	35.58
-92.5	38.25	40.60
-95.0	39.73	40.78
-97.5	38.07	38.02
-100.0	39.44	39.62
-102.5	40.48	40.52
-105.0	41.06	41.07

The drawback of the MVSCG algorithm is the high computational burden of its training procedure, which can be prohibitive in real-time applications, despite the low cost achieved by using methods such as that in [28]. To tackle this impairment, it is suggested that the MVSCG algorithm be used only at an initialization stage. Thereafter, it is recommended that the low computational cost first-order training procedure suggested in [29] be used. Computer simulations have revealed that this strategy is appropriate to overcome the high complexity demanded by the MVSCG training algorithm at a cost of low-performance degradation.

To assess the effects of the improved SNR in the system performance, Tables III and IV show the achievable bit rate, in megabits per second, for both PL channels. These results were obtained considering  $\Gamma = 9.8$  dB, to guarantee that  $P_e = 10^{-6}$ ,  $\gamma_m = 6$  dB,  $\gamma_c = 3$  dB;  $v = 16$ ; and  $L_w = 48$  and  $L_w = 56$  for PL channels 1 and 2, respectively. The min-ISI [24] channel-shortening equalizer was used to obtain these results. It can be observed in Tables III and IV that in the presence of high-power impulse noise, significant improvements in the achievable bit rate are obtained.

Figs. 8 and 9 illustrate the achievable bit rate versus the length of the shortening equalizer for both PL channels. These figures show the performance of the proposed M-PLC-DMT against

TABLE IV  
PL CHANNEL 2: M-PLC-DMT AND PLC-DMT PERFORMANCE UNDER DIFFERENT IMPULSE NOISE PSD LEVELS

PSD(dB/Hz)	Bit-rate (Mbps) PLC-DMT	Bit-rate (Mbps) M-PLC-DMT
-90.0	26.10	30.78
-92.5	29.81	35.48
-95.0	34.60	41.39
-97.5	35.85	36.42
-100.0	37.41	38.24
-102.5	39.70	39.94
-105.0	41.01	41.15

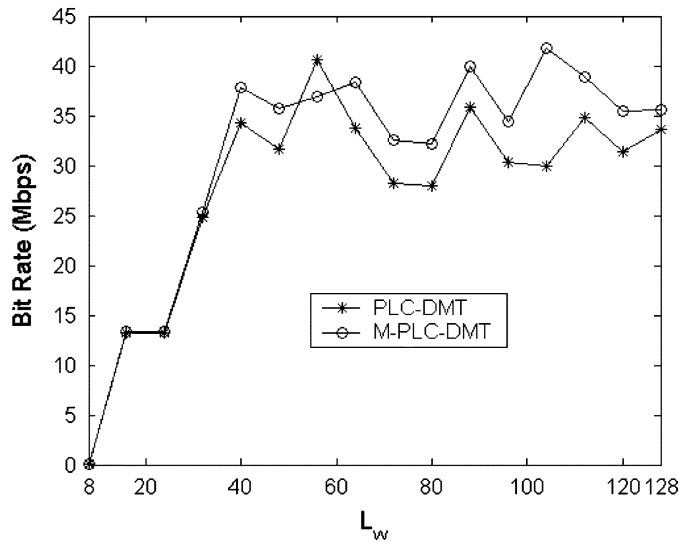


Fig. 8. M-PLC-DMT and PLC-DMT performances in terms of the length of a shortening equalizer for PL channel 1 when  $v = 16$ .

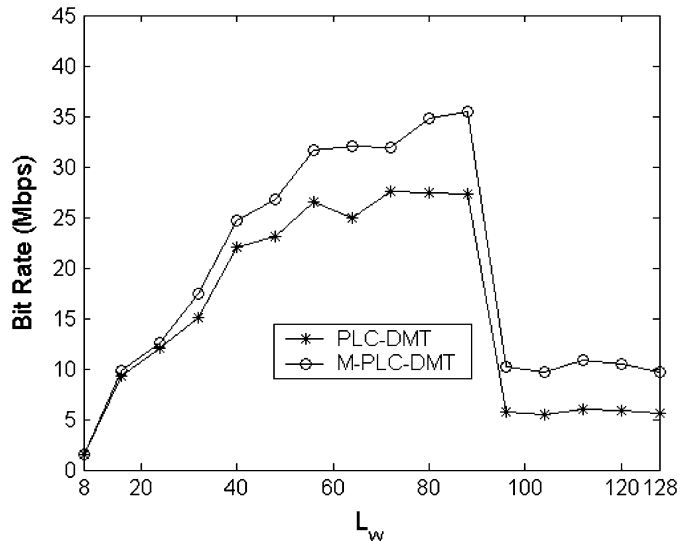


Fig. 9. M-PLC-DMT and PLC-DMT performances in terms of the length of a shortening equalizer for PL channel 2 when  $v = 16$ .

PLC-DMT when the length of the shortening equalizer varies from 8 to 128. The following were used to obtain these figures: the PSD of transmitted signal, impulse noise, and background noise are equal to  $-70$  dB/Hz,  $-90$  dB/Hz, and  $-120$  dB/Hz, respectively;  $\Gamma = 9.8$  dB;  $P_e = 10^{-6}$ ;  $\gamma_m = 6$  dB;  $\gamma_c = 3$  dB. As can be seen in Figs. 8 and 9, the M-PLC-DMT attains a

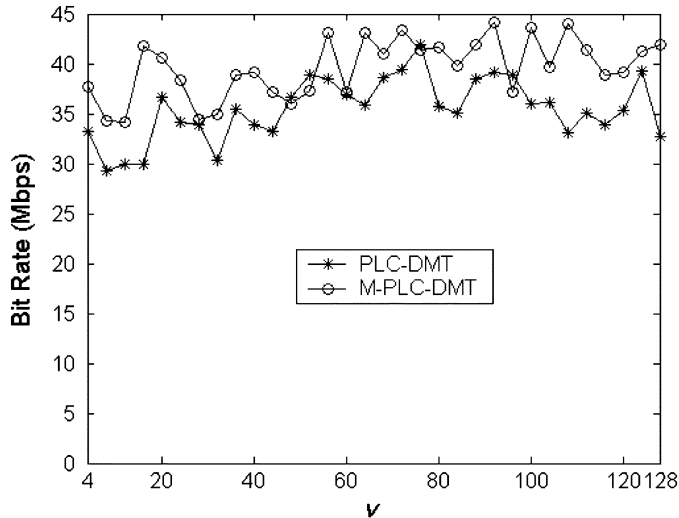


Fig. 10. M-PLC-DMT and PLC-DMT performances in terms of  $\nu$  for PL channel 1 when  $L_w = 104$ .

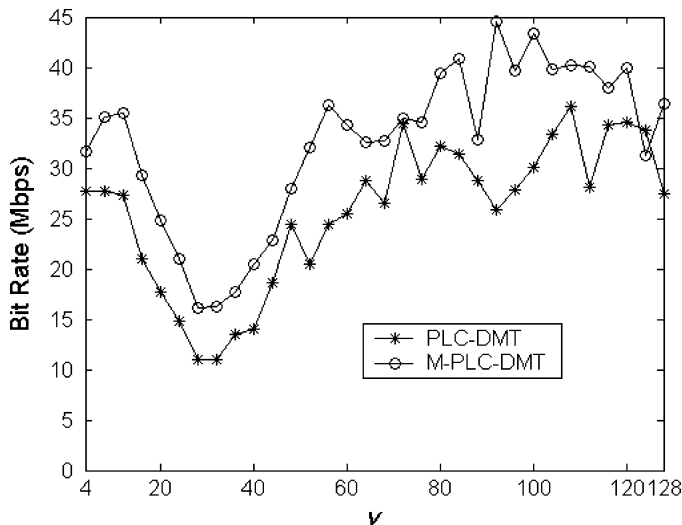


Fig. 11. M-PLC-DMT and PLC-DMT performances in terms of  $\nu$  for PL channel 2 when  $L_w = 88$ .

higher bit rate than the PLC-DMT. For these PL channels, the improvement exceeds 20% for  $L_w = 104$ .

Finally, Figs. 10 and 11 display the performance of PLC-DMT and M-PLC-DMT when  $\nu$  is fixed and  $L_c$  varies from 4 to 128. Both figures highlight the fact that M-PLC-DMT attains a higher data rate than PLC-DMT. To get these results, the same parameters used for obtaining the results shown in Figs. 9 and 10 were used.

## V. CONCLUDING REMARKS

This contribution has proposed the M-PLC-DMT, a modified version of the traditional PLC-DMT solution. Basically, the use of an MLPNN before the TEQ has been included to provide impulse noise reduction and, consequently, enhance the SNR in each subchannel. The improvements on the achieved bit rates have been verified under different conditions. The simulation results reveal that the proposed method has a notable effectiveness under high-impulse-noise presence.

Although the proposed M-PLC-DMT solution presents remarkable results under the impulse noise presence in LVDN, the analysis of other kinds of computational intelligence techniques associated with other optimization methods may show a better tradeoff between the computational complexity and performance for real-time implementation. The authors are currently investigating this topic.

## ACKNOWLEDGMENT

The authors would like to thank Prof. S. K. Mitra and P. N. S. Ribeiro for their valuable suggestions and corrections when proofreading this contribution. The authors also thank the anonymous reviewers for providing valuable comments and suggestions.

## REFERENCES

- [1] N. Pavlidou, A. J. Han Vinck, J. Yazdani, and B. Honary, "Power line communications: State of art and future trends," *IEEE Commun. Mag.*, vol. 41, no. 4, pp. 34–40, Apr. 2003.
- [2] Y.-J. Lin, H. A. Latchman, M. Lee, and S. Katar, "A power line communication network infrastructure for the smart home," *IEEE Wireless Commun.*, vol. 9, no. 6, pp. 104–111, Dec. 2002.
- [3] Y.-J. Lin, H. A. Latchman, R. E. Newman, and S. Katar, "A comparative performance study of wireless and power line networks," *IEEE Commun. Mag.*, vol. 41, no. 4, pp. 54–63, Apr. 2003.
- [4] J. Abad, A. Badenes, J. Blasco, J. Carreras, V. Dominguez, C. Gomez, S. Iranzo, J. C. Riveiro, D. Ruiz, L. M. Torres, and J. Comabella, "Extending the power line LAN up to the neighborhood transformer," *IEEE Commun. Mag.*, vol. 41, no. 4, pp. 64–70, Apr. 2003.
- [5] G. Jee, C. Edison, R. D. Rao, and Y. Cern, "Demonstration of the technical viability of PLC systems on medium- and low-voltages lines in the United States," *IEEE Commun. Mag.*, vol. 41, no. 5, pp. 108–112, May 2003.
- [6] K. Dostert, *Power Line Communications*. Upper Saddle River, NJ: Prentice-Hall, 2001.
- [7] P. J. Langfeld, "The capacity of typical power line reference channels and strategies for system design," in *Proc. 5th Power-Line Communication Applications, Int. Symp.*, 2001, pp. 271–278.
- [8] W. Sanderson, "Broadband communications over a rural power distribution circuit," in *Proc. IEEE Southeastcon*, 2000, pp. 497–504.
- [9] H. Dai and H. V. Poor, "Advanced signal processing for power line communications," *IEEE Commun. Mag.*, vol. 41, no. 5, pp. 100–107, May 2003.
- [10] E. Biglieri, "Coding and modulation for a horrible channel," *IEEE Commun. Mag.*, vol. 41, no. 5, pp. 92–98, May 2003.
- [11] S. Baig and N. D. Gohar, "A discrete multitone transceiver at the heart of the PHY layer of an in-home power line communication local-area network," *IEEE Commun. Mag.*, vol. 41, no. 4, pp. 48–53, Apr. 2003.
- [12] M. B. Loiola, M. V. Ribeiro, and J. M. T. Romano, "A turbo equalizer using fuzzy filters," in *Proc. IEEE Machine Learning for Signal Processing Workshop*, 2004, pp. 695–704.
- [13] M. V. Ribeiro, "Learning rate updating methods applied to adaptive fuzzy equalizers for broadband power line communications," *EURASIP J. Appl. Signal Process., Special Issue Signal Image Process.*, vol. 16, pp. 2592–2599, 2004.
- [14] L. M. Reyneri, "Unification of neural and wavelet networks and fuzzy systems," *IEEE Trans. Neural Netw.*, vol. 10, no. 4, pp. 801–814, Jul. 1999.
- [15] J. G. Proakis, *Digital Communications*, 4th ed. New York: McGraw-Hill, 2000.
- [16] T. Starr, J. M. Cioffi, and P. J. Silverman, *Understanding Digital Subscriber Line Technology*. Upper Saddle River, NJ: Prentice-Hall, 1998.
- [17] M. Zimmermann and K. Dostert, "A multipath model for the powerline channel," *IEEE Trans. Commun.*, vol. 50, no. 4, pp. 553–559, Apr. 2002.
- [18] I. Kalet, "The multitone channel," *IEEE Trans. Commun.*, vol. 37, no. 2, pp. 119–124, Feb. 1989.
- [19] J. A. C. Bingham, "Multicarrier modulation for data transmission: An idea whose time has come," *IEEE Commun. Mag.*, vol. 28, no. 5, pp. 5–14, May 1990.

- [20] M. V. Ribeiro, C. A. Duque, and J. M. T. Romano, "Implementação computacional de um simulador para transmissão broadband via canais PLC," in *Proc. XVIII NPTEE XVII Seminário Nacional de Produção e Transmissão de Energia Elétrica*, 2003, pp. GTL 1–GTL 6. (in Portuguese).
- [21] W. Liu, H. Widmer, and P. Raffin, "Broadband PLC access systems and field deployment in European power line networks," *IEEE Commun. Mag.*, vol. 41, no. 5, pp. 114–118, May 2003.
- [22] M. Zimmermann and K. Dostert, "Analysis and modeling of impulse noise in broad-band powerline communications," *IEEE Trans. Electromagn. Compat.*, vol. 44, no. 1, pp. 249–258, Feb. 2002.
- [23] J. A. C. Bingham, *ADSL, VDSL, and Multicarrier Modulation*. New York: Wiley, 2000.
- [24] G. Arslan, B. L. Evans, and S. Kiaei, "Equalization for discrete multitone transceivers to maximize bit-rate," *IEEE Trans. Signal Processing*, vol. 49, no. 12, pp. 3123–3135, Dec. 2001.
- [25] X.-P. Zhang, "Thresholding neural network for adaptive noise reduction," *IEEE Trans. Neural Netw.*, vol. 12, no. 3, pp. 567–584, May 2001.
- [26] E. P. Santos and F. J. Von Zuben, "Efficient second-order learning algorithm for discrete-time recurrent neural networks," in *Recurrent Neural Networks: Design and Applications*, L. Medsker and L. C. Jain, Eds. Boca Raton, FL: CRC, 2000, pp. 47–75.
- [27] M. V. Ribeiro, J. G. A. Barbedo, J. M. T. Romano, and A. Lopes, "Fourier-lapped-multilayer perceptron (FLMLP) method for speech quality assessment," *EURASIP J. Appl. Signal Processing, Special Issue on Anthropomorphic Processing Audio Speech*, vol. 9, pp. 1425–1434, 2005.
- [28] B. A. Pearlmutter, "Fast exact multiplication by the Hessian," *Neural Comput.*, vol. 6, no. 1, pp. 147–160, 1994.
- [29] M. N. Vrahatis, G. D. Magoulas, and V. P. Plagianakos, "Globally convergent modification of the quickprop method," *Neural Processing Lett.*, vol. 12, pp. 159–169, 2000.
- [30] J. A. Bingham and F. Van Der Putten, T1.413 Issue 2: Standards Project for Interfaces Relating to Carrier to Customer Connection of Asymmetrical Digital Subscriber Line (ADSL) Equipment, Sep. 1997. ANSI document, no. T1E1.4/97-007R6.
- [31] M. V. Ribeiro, "Signal processing techniques for power line communication and power quality applications," Ph.D. thesis (in Portuguese), Dept. Commun., Univ. Campinas, Campinas, Brazil, 2005.



**Moisés V. Ribeiro** (S'03–M'05) was born in Três Rios, Brazil, in 1974. He received the B.S. degree in electrical engineering from the Federal University of Juiz de Fora (UFJF), Juiz de Fora, Brazil, in 1999, and the M.Sc. and Ph.D. degrees in electrical engineering from the University of Campinas (UNICAMP), Campinas, Brazil, in 2001 and 2005, respectively.

He was a Postdoctoral Researcher at UNICAMP in 2005. Currently, he is a Visiting Professor at UFJF.

He was a Visiting Researcher in the Image and Signal Processing Laboratory of the University of California, Santa Barbara, in 2004. His research interests include filter banks, computational intelligence, digital and adaptive signal processing applied to power quality, power-line communication, multimedia, and biomedical applications. He has been the recipient of nine scholarships from the Brazilian government agencies, and is the author of nine journal and 26 conference papers. He holds six patents.

Dr. Ribeiro received student awards from IECON'01 and ISIE'03.



**Renato da R. Lopes** received the B.S. and M.S. degrees in electrical engineering from the University of Campinas (UNICAMP), Campinas, Brazil, in 1995 and 1997, and the Ph.D. degree in electrical engineering from the Georgia Institute of Technology (GT), Atlanta, in 2003.

He was a Teaching Assistant with UNICAMP in 1996. He held teaching and research assistant positions from 1999 to 2003 at GT. From 2003 to 2005, he was a Postdoctoral Researcher with the Signal Processing for Communications Research Group at UNI-

CAMP, under a grant from FAPESP. Currently, he is an Assistant Professor with the School of Electrical and Computer Engineering, UNICAMP. His research interests are in the general area of communications theory, including equalization, identification, iterative receivers, and coding theory.



**João Marcos T. Romano** (M'88–SM'02) was born in Rio de Janeiro, Brazil, in 1960. He received the B.S. and M.S. degrees in electrical engineering from the University of Campinas (UNICAMP), Campinas, Brazil, in 1981 and 1984, respectively, and the Ph.D. degree from the University of Paris-XI, Paris, France, in 1987.

Currently, he is a Professor with the Communications Department of the Faculty of Electrical and Computer Engineering at UNICAMP, where he has been since 1988. He was an Invited Professor with the

University René Descartes, Paris, in 1999, and in the Communications and Electronic Laboratory, Conservatoire National des Arts et Métiers (CNAM), Paris, in 2002. He is responsible for the Signal Processing for Communications Laboratory at UNICAMP. He has been the Vice-Director of the School of Electrical and Computer Engineering of UNICAMP since 2003. His research interests include adaptive and intelligent signal processing and its applications in telecommunications problems, such as channel equalization and smart antennas.

Dr. Romano was the President of the Brazilian Communications Society (SBrT), a sister society of ComSoc-IEEE, from 2000 to 2004. He has been a recipient of the Research Fellowship of CNPq-Brazil since 1988.

**Carlos A. Duque** (M'91) was born in Juiz de Fora, Brazil, in 1962. He received the B.S. degree in electrical engineering from the Federal University of Juiz de Fora, Juiz de Fora, Brazil, in 1986, and the M.Sc. and Ph.D. degrees in electrical engineering from the Catholic University of Rio de Janeiro, Rio de Janeiro, Brazil, in 1990 and 1997, respectively.

He has been a Professor in the Engineering Faculty at Federal University of Juiz de Fora (UFJF), Juiz de Fora, Brazil, since 1989. His research interests are power-quality analysis, digital instrumentation, and digital signal processing.